

See discussions, stats, and author profiles for this publication at: <https://www.researchgate.net/publication/224817096>

Comparison between the LCST and UCST Transitions of Double Thermoresponsive Diblock Copolymers: Insights into the Behavior of POEGMA in Alcohols

ARTICLE *in* MACROMOLECULES · APRIL 2012

Impact Factor: 5.8 · DOI: 10.1021/ma300374y

CITATIONS

40

READS

96

3 AUTHORS:



[Peter J. Roth](#)

Curtin University

51 PUBLICATIONS 1,062 CITATIONS

SEE PROFILE



[Thomas P Davis](#)

Monash University (Australia)

498 PUBLICATIONS 19,763 CITATIONS

SEE PROFILE



[Andrew B. Lowe](#)

Curtin University

175 PUBLICATIONS 8,750 CITATIONS

SEE PROFILE

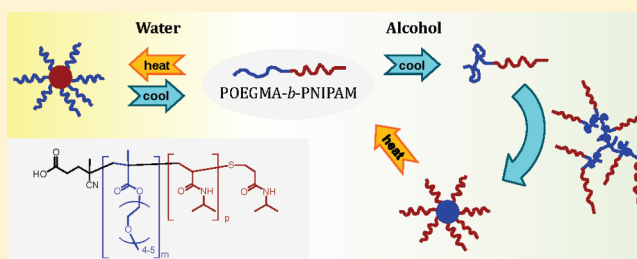
Comparison between the LCST and UCST Transitions of Double Thermoresponsive Diblock Copolymers: Insights into the Behavior of POEGMA in Alcohols

Peter J. Roth, Thomas P. Davis,* and Andrew B. Lowe*

Centre for Advanced Macromolecular Design (CAMD), School of Chemical Engineering, University of New South Wales, Kensington, Sydney, New South Wales 2052, Australia

S Supporting Information

ABSTRACT: Doubly thermoresponsive polymers consisting of a poly[oligo(ethylene glycol) methyl ether methacrylate] (POEGMA) block displaying UCST behavior in alcohols and a block of poly(*N*-isopropylacrylamide) (PNIPAM) or poly(*N,N*-diethylacrylamide) (PDEAM), each of which has an LCST in water, were synthesized using RAFT polymerization followed by simultaneous activated ester/amine and nucleophilic thiol–ene postpolymerization conversions. Upon heating aqueous solutions of POEGMA-*b*-PNIPAM, ¹H NMR spectroscopy confirmed a sudden decrease of the PNIPAM signals at the LCST, indicating dehydration and chain collapse. Dynamic light scattering (DLS) and turbidity measurements observed the macroscopic phase separation of the PNIPAM block at the same temperature. In 2-propanol, ¹H NMR spectroscopy showed a gradual decrease of the POEGMA signals over a range of more than 30 °C during its UCST transition, indicating early stages of chain crumpling up to 20 °C above the macroscopic phase separation. The OEG side chains were found to collapse onto the backbone starting at the ester linkages, indicating the most unfavorable enthalpic polymer–solvent interactions occur adjacent to the ester group. Although the diblock copolymers displayed a strong concentration-dependent cloud point, ¹H NMR spectroscopy revealed a concentration-independent desolvation, indicating the potential for applications that are not based on phase separation but on changes of polymer conformation. The phase separation occurred within a narrow temperature range of ~6 °C as evidenced by turbidity and DLS. This transition could be exploited to self-assemble POEGMA-*b*-PDEAM into micellar structures with POEGMA cores in 1-octanol. Cooling to ~15 °C below the cloud point was necessary to produce compact structures. Upon heating, the aggregates remained compact until redissolving entirely within a range of 1 °C, making the UCST of POEGMA in alcohols a valuable tool for reversible self-assembly applications.



INTRODUCTION

Thermally responsive, smart materials have been receiving significant attention from various research fields including bioconjugate chemistry,¹ biomedicine,² sensors,^{3–5} molecular actuators,⁶ and separation technology.⁷ The majority of these polymers display an LCST-type transition in aqueous solution; i.e., they phase separate upon heating. Prominent examples are poly(*N*-isopropylacrylamide) (PNIPAM, LCST_{H₂O} ~ 32 °C),⁸ poly(*N,N*-diethylacrylamide) (PDEAM, LCST_{H₂O} ~ 33 °C),⁹ and various (meth)acrylic poly(ethylene glycol) (PEG) analogues, such as poly[oligo(ethylene glycol) methyl ether methacrylate] (*M*_{monomer} ~ 300 g/mol) (POEGMA, LCST_{H₂O} ~ 64 °C).^{10–13} The opposite, UCST-type behavior involving phase separation upon cooling is less common in polar solvents. Examples of polysulfobetaines^{14,15} and certain amide functional polymers^{16–19} display UCSTs in water, while poly(methyl methacrylate)^{4,20} and some polyoxazolines^{21,22} display UCSTs in water/alcohol mixtures. POEGMA was recently shown to undergo UCST transitions in aliphatic alcohols with the critical temperature increasing strongly with

an increasing alcohol chain length.²³ Pioneered by Armes^{24,25} and Laschewsky,^{26,27} doubly thermoresponsive diblock copolymers consisting of an LCST-type and a UCST-type block have been employed for the temperature-controlled formation of micelles and inverted micelles.^{21,28–33}

Although often considered direct opposites, LCST and UCST transitions have quite different theoretical foundations.³⁴ According to the solution theory by Flory and Huggins, a phase separation can only occur in a system featuring unfavorable enthalpic interactions between polymer segments and solvent molecules. In such a case the mixing entropy will still outbalance the positive enthalpy at low polymer concentrations. At thermodynamic equilibrium, a mixture of a very small amount of polymer in a very large amount of solvent will therefore consist of a single phase. For a given nonextreme concentration the type of phase transition (LCST or UCST) then depends on the temperature dependence of the mixing

Received: February 22, 2012

Revised: March 18, 2012

Published: April 2, 2012

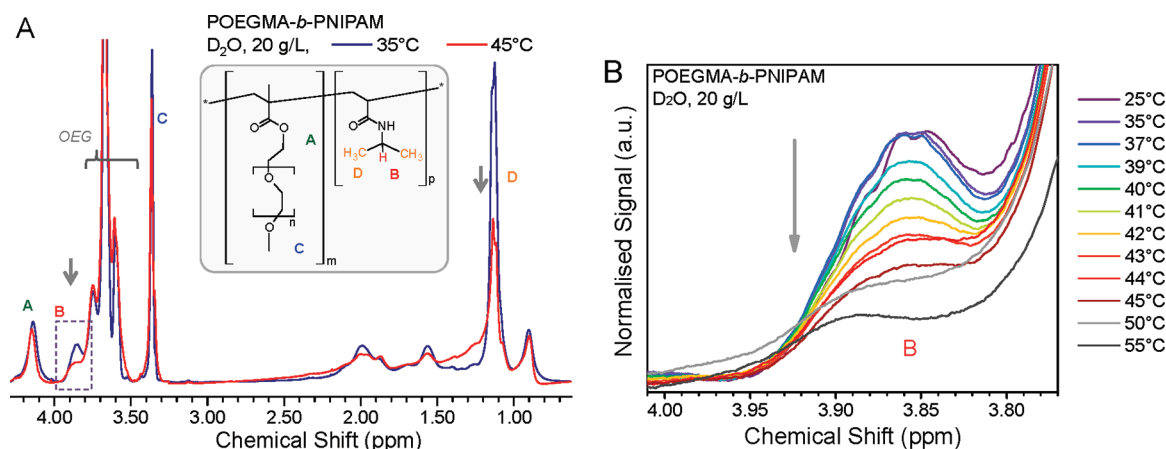


Figure 1. Variable temperature ¹H NMR measurements of POEGMA-*b*-PNIPAM in D₂O. (A) Overlay of NMR spectra at 35 and 45 °C showing the decrease and broadening of the PNIPAM signals above the critical temperature. (B) Section (dashed rectangle in part A) showing the decrease of the *N*-isopropylmethine proton with increasing temperature.

enthalpy or the associated interaction parameter χ . For an LCST transition, χ increases with temperature, making the polymer solvophobic above a critical temperature. The phase transition is driven by a gain of overall entropy when the dense, highly ordered solvation shell around the polymer is released into bulk water. LCST transitions usually occur sharply, and the critical temperatures of polymers such as PNIPAM³⁵ or POEGMA¹³ in water have been shown to display very low concentration dependences. A UCST type transition, on the other hand, can occur when χ is positive and does not vary strongly with temperature. Upon cooling a solution, the entropic contribution favoring a mixing gradually decreases, allowing the unfavorable enthalpic term to dominate, which causes a phase separation. Pietsch, Hoogenboom, and Schubert recently exploited the gradual UCST transition of PMMA in ethanol/water for temperature sensing. The authors incorporated solvatochromic dyes into PMMA which allowed for a sensing regime of ~ 30 °C while the PMMA chains gradually became insoluble upon cooling.⁴

As a PEG analogue, POEGMA is an interesting material not just because of its tunable LCST and UCST behaviors but also because of its well-established biocompatibility and non-toxicity.^{11,12,36} The UCST behavior in alcohols presents a promising opportunity for directed self-assembly potentially leading to structures that might not be available easily through other techniques. However, apart from basic turbidity measurements, the solution properties of POEGMA in alcohols have not been further characterized. Whereas LCST-type polymers are frequently employed in thermally triggered self-assembly, the exploitation of the UCST of POEGMA in alcohols represents a complementary trigger for self-directed assembly that should be considered.

NMR spectroscopy is an expedient method for the observation of phase transitions of polymers and is routinely used to study LCST transitions of (co)polymers and mixtures thereof.^{37–39} Through a broadening and disappearance of peaks, ¹H NMR spectroscopy gives direct information on the solvation of discrete structural units of (co)polymers. NMR spectroscopy has also been shown to be an alternative method to dynamic light scattering for verifying the self-assembly of pH responsive copolymers.⁴⁰

Herein, we report on the synthesis of two diblock copolymers, POEGMA-*b*-PNIPAM and POEGMA-*b*-PDEAM,

employing a combination of RAFT polymerization and the activated ester/amine and thiol–ene conjugation concepts. POEGMA is completely soluble in water during the LCST transitions of PNIPAM and PDEAM, while the latter two species remain soluble in 2-propanol in which POEGMA displays a UCST transition. Using these doubly thermoresponsive copolymers, we investigated the phase transitions in (deuterated) water and 2-propanol by ¹H NMR spectroscopy, turbidity, and DLS. In each case, the soluble blocks stabilized aggregates and served as an internal reference in the NMR experiments. Insights into the gradual desolvation of the POEGMA blocks during its UCST transition and a direct comparison with the prototypical smart polymer PNIPAM were possible on the same AB diblock copolymer. Concentration-dependent measurements showed that the phase transition cannot be observed by NMR spectroscopy and suggested that chain collapse and phase separation should be regarded separately for POEGMA in alcohols. Finally, implications of the gradual UCST transition and the potential for self-assembly were investigated in 1-octanol.

EXPERIMENTAL SECTION

Methods. Size exclusion chromatography (SEC) was performed on a Shimadzu system with four phenogel columns in THF operating at a flow rate of 1 mL/min. Chromatograms were analyzed by Cirrus SEC software version 3.0. The system was calibrated with a series of narrow molecular weight distribution polystyrene standards with molecular weights ranging from 0.58 to 1820 kg/mol.

Dynamic light scattering (DLS) measurements were performed on a Malvern Zetasizer Nano ZS at a scattering angle of 173° and analyzed by Malvern Zetasizer Software version 6.20. Measurements in alcohols were corrected for temperature-dependent viscosities for each temperature individually using the empirical relation $\eta(2\text{-propanol}) = 10^{[-0.7009 + 841.50 \times T^{-1} - 6.068 \times 10^{-3} \times T + 8.2964 \times 10^{-6} \times T^2]}$ ⁴¹ and $\eta(1\text{-octanol}) = 9.653 \times 10^{-3} \times \exp[811.748 \times T^{-1} + 346920 \times T^{-2}]$,⁴² where η is the viscosity in cP and T is the temperature in K.

NMR spectroscopic measurements were performed on a Bruker DPX 300 instrument and evaluated using MestReC 4.7.0.0 software. For measurements in CDCl₃, the internal solvent signal was used as a standard ($\delta = 7.260$ ppm). For measurements at variable temperatures in 2-propanol-*d*₈, the residual solvent signal of the methyl groups was set to 1.095 ppm. Samples were cooled and allowed to equilibrate at each temperature for at least 15 min prior to measurement. Curves at each temperature were normalized to the integral of the residual OH solvent signal. Integrals were evaluated in the following limits (see

Figure 1 for assignment): oligo ethylene glycol (OEG) methylene (A) 4.265–4.060 ppm; CHMe₂ (B) 4.060–3.923 ppm; OEG 3.858–3.470 ppm, OEG methoxy (C) 3.470–3.278 ppm. Values were plotted relative to the integrals at 30 °C which were normalized to 100%. Measurements at variable temperatures in D₂O were performed by heating samples and allowing them to equilibrate for at least 15 min at each temperature prior to measurements. Because of the shifting of the internal HDO resonance signal with temperature the chemical shift of the OEG-methoxy group was used as a reference and set to 3.360 ppm at each temperature, in good agreement with the chemical shifts observed in CDCl₃ and 2-propanol-*d*₈. The curves were normalized to the integral of the OEG methyl group in the limits of 3.420–3.300 ppm, which therefore remained constant with temperature. The integral of the *N*-isopropylmethine group in the limits of 3.950–3.812 ppm was plotted relative to its value at 25 °C which was normalized to 100%.

Transmission electron microscopy (TEM) was performed on a Jeol 1400 instrument with an accelerating voltage of 100 kV. Samples in cold 1-octanol were prepared by cooling a solution (5.0 g/L) to 0 °C, dropping two drops onto a carbon-coated TEM grid on a tissue and letting it dry for 1 week in the fridge.

Turbidity measurements were performed on a Varian Cary 300 Scan spectrophotometer equipped with a Cary temperature controller and a Peltier heating element in quartz cuvettes of 10 mm path length at a wavelength of 520 nm. Heating rates were 1 °C/min for all measurements except for POEGMA-*b*-PNIPAM in D₂O at 20 g/L

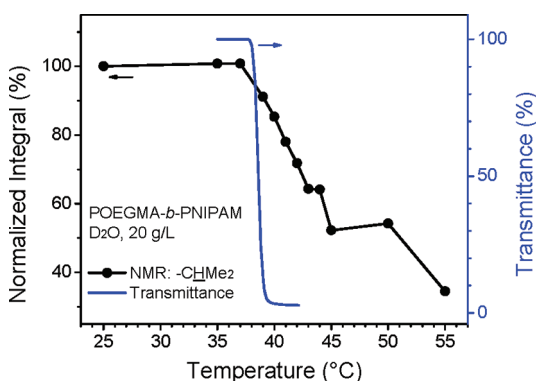


Figure 2. Relative decrease of the NMR integral of the *N*-isopropylmethine hydrogen in POEGMA-*b*-PNIPAM upon heating (black curve, left axis) and turbidity measurement (blue curve, right axis) showing the concomitant dehydration on a molecular level and clouding of the solution.

(Figure 2) which was heated at 0.1 °C/min to minimize a heating rate shift. For clear solutions (cold water; warm alcohol) the baseline was corrected to zero absorbance, A . Transmittance, $T = 10^{-A}$, was plotted against temperature, and cloud points were determined at 50% transmittance or at the average of maximal and minimal transmittance for samples of which the transmittance did not decrease to ~0%.

Materials. All chemicals were purchased from Sigma-Aldrich at the highest available purity and used as received unless stated otherwise. Oligo(ethylene glycol) methyl ether methacrylate with an average M_n of 300 g/mol (OEGMA) was filtered through basic alumina to remove stabilizers. 2,2'-Azobis(isobutyronitrile) (AIBN) was recrystallized from methanol and stored at -25 °C until needed. 4-(4-Cyanopentanoic acid) dithiobenzoate (CPADB)⁴³ and pentafluorophenyl acrylate (PFPA)⁴⁴ were synthesized following literature procedures.

Synthesis of Poly[oligo(ethylene glycol) methyl ether methacrylate] (POEGMA). 2.25 g (7.5 mmol) of OEGMA, 8.2 mg (0.05 mmol) of AIBN, 83.7 mg of CPADB (0.3 mmol), and 3.0 mL of DMF were combined in a round-bottom flask which was capped with a rubber septum and nitrogen was bubbled through the solution for 20 min. The flask was then placed into a preheated oil bath at 80 °C and

stirred overnight. POEGMA was isolated by precipitation into hexane. Yield 1.65 g (73%). M_n (SEC) = 6.3 kg/mol, PDI (SEC) = 1.18. ¹H NMR (CDCl₃) δ /ppm = 4.06 (bs, 2 H, -C(=O)OCH₂-), 3.73–3.45 (m, ~15 H, OEG), 3.36 (bs, 3 H, OEG-CH₃), 2.06–0.65 (m, 5 H, backbone).

Poly[oligo(ethylene glycol) methyl ether methacrylate]-*b*-poly(pentafluorophenyl acrylate) (POEGMA-*b*-PPFPA). POEGMA-*b*-PPFPA was prepared following a literature procedure.⁴⁵ Briefly, POEGMA was used as a macro-CTA for the polymerization of PFPA. The product POEGMA-*b*-PPFPA was isolated by precipitation into hexane. M_n (SEC) = 14.8 kg/mol, PDI (GPC) = 1.37. ¹H NMR (CDCl₃) δ /ppm = 4.08 (bs, 2 H, -C(=O)OCH₂-), 3.81–3.50 (m, ~15 H, OEG), 3.38 (bs, 3 H, OEG-CH₃), 2.93–0.65 (m, backbone). ¹⁹F NMR (CDCl₃) δ /ppm = -153.6 (bs, 2 F, ortho), -157.1 (bs, 1 F, para), 162.6 (bs, 2 F, meta)

Conversion of POEGMA-*b*-PPFPA into POEGMA-*b*-PNIPAM and POEGMA-*b*-PDEAM. 292 mg of POEGMA-*b*-PPFPA was dissolved in 5.0 mL of THF. 416 μ L of isopropylamine or 560 μ L of diethylamine (5.41 mmol) and 113 μ L of triethylamine (0.81 mmol) were added, and the mixtures stirred at RT overnight. 200 μ L of the reaction mixture was taken out and diluted with 450 μ L of CDCl₃ for ¹⁹F NMR analysis which showed the complete disappearance of the PFP ester peaks and instead the signals of free PFP-OH at δ /ppm = -170.4 (2 F, ortho), -171.5 (2 F, meta), and -189.1 (1 F, para). The NMR samples were recombined with the reaction mixtures and purified by dialysis against methanol in 3500 g/mol MWCO regenerated cellulose membranes for 3 days with solvent changes twice per day. The solvent was removed, a small amount of water was added, and the products were freeze-dried.

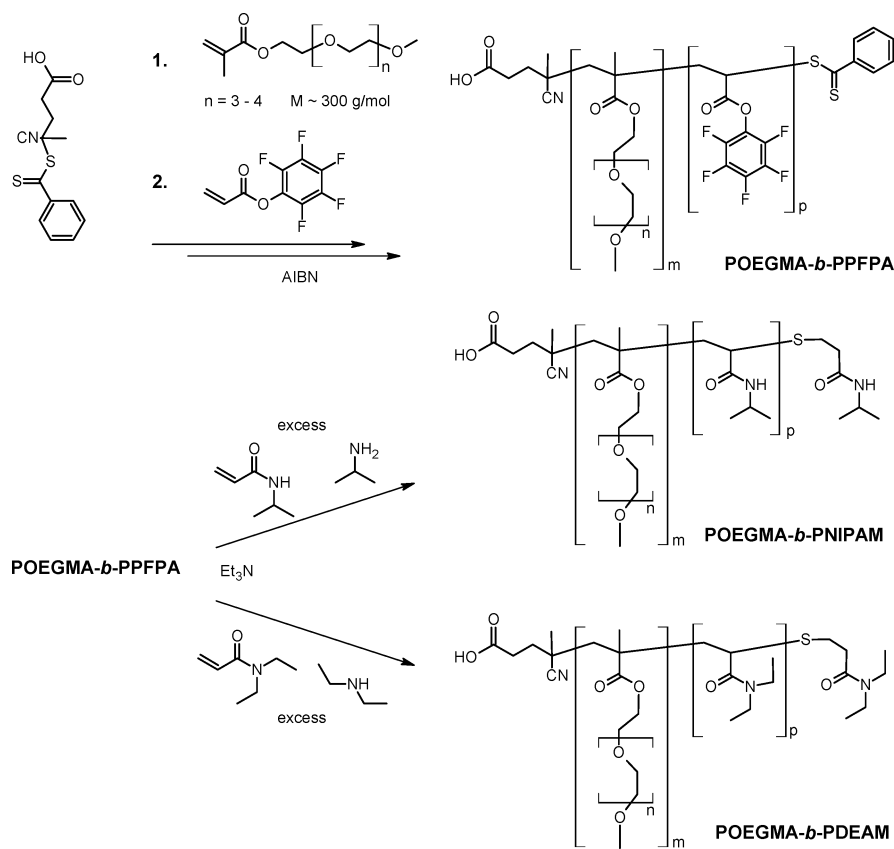
POEGMA-*b*-PNIPAM. Yield 184.8 mg (91%), M_n (SEC) = 12.3 kg/mol, PDI (GPC) = 1.22. ¹H NMR (CDCl₃) δ /ppm = 4.08 (bs, -C(=O)OCH₂-), 3.98 (bs, -NHCH(CH₃)₂), 3.81–3.47 (m, OEG), 3.37 (bs, OEG-CH₃), 3.00–0.65 (m, backbone), 1.12 (bs, -NHCH(CH₃)₂). ¹⁹F NMR (CDCl₃): no signals.

POEGMA-*b*-PDEAM. Yield 206.7 mg (92%), M_n (SEC) = 11.5 kg/mol, PDI (SEC) = 1.16. ¹H NMR (CDCl₃) δ /ppm = 4.08 (bs, -C(=O)OCH₂-), 3.80–2.95 (m, OEG, -N(CH₂CH₃)₂), 2.95–0.65 (m, backbone), 1.07 (bs, -N(CH₂CH₃)₂). ¹⁹F NMR (CDCl₃): no signals.

RESULTS AND DISCUSSION

Synthesis. An overview of the synthesis of the target diblock copolymers is given in Scheme 1. Reversible addition–fragmentation chain transfer (RAFT) polymerization of oligo(ethylene glycol methyl ether) methacrylate (OEGMA, monomer molecular weight = 300 g/mol) was employed to prepare a macro-RAFT agent with a molecular weight of 6.3 kg/mol and a PDI of 1.18. A sequential RAFT polymerization with pentafluorophenyl acrylate (PFPA) was used to prepare the diblock copolymer POEGMA-*b*-PPFPA with a molecular weight of 14.8 kg/mol and a PDI of 1.37. SEC showed a shift of the entire POEGMA peak toward higher molecular weight, as shown in Figure S1 of the Supporting Information, confirming successful block copolymer formation. In a subsequent postpolymerization modification, the activated PFP esters of the second block were converted into amides with either *N*-isopropylamine or *N,N*-diethylamine. Simultaneously, the dithioester end groups of the AB diblock copolymer were aminolyzed, and the resulting thiols were reacted in situ with *N*-isopropylacrylamide or *N,N*-diethylacrylamide in nucleophilic thiol–ene reactions.^{46–48} This procedure avoided side reactions of the terminal thiols, e.g. oxidative coupling, and produced end groups that were chemically indistinct from the repeat units of the second block. The influence of end groups on the thermal behavior of the copolymers in water or alcohols could thus be neglected. The conversion of the PFP esters with amines to give amides was followed by ¹⁹F NMR spectroscopy. The complete absence of fluorine signals confirmed the successful

Scheme 1. Synthesis of POEGMA-*b*-PNIPAM and POEGMA-*b*-PDEAM by RAFT Polymerization and Subsequent Simultaneous Activated Ester/Nucleophilic Thiol–Ene Chemistry



aminolysis of the esters followed by a complete removal of the pentafluorophenol side product by dialysis (see Figure S2). The postpolymerization approach thus enabled the synthesis of two diblock copolymers with the same degrees of polymerization. POEGMA-*b*-PNIPAM was found to have a molecular weight of 12.3 kg/mol with a PDI of 1.22, while the sister polymer POEGMA-*b*-PDEAM had a molecular weight of 11.5 kg/mol and a PDI of 1.16. Both copolymers had similar weight ratios of each block. SEC traces, shown in Figure S1, showed monomodal size distributions and low PDIs, indicating that no disulfide coupling had taken place during aminolysis.

Solution Behavior in Water. The thermally triggered micellization of diblock copolymers consisting of a soluble block and an LCST-type block—especially PNIPAM—is a well-established technique.⁴⁹ Here, the solution behavior in water is briefly discussed to confirm the expected collapse of the PNIPAM block and to provide a direct comparison for the behavior of the diblock copolymers in alcohol. POEGMA-*b*-PNIPAM was analyzed by variable temperature ¹H NMR spectroscopic measurements at a concentration of 20 g/L in D₂O. Spectra measured at 35 and 45 °C are shown in Figure 1A. At 35 °C (blue spectrum) the PNIPAM block had not collapsed yet—seen from a comparison with a spectrum measured in CDCl₃ and from turbidity data discussed below. The increase of the phase transition temperature compared to the well-documented value of 32 °C, known for PNIPAM homopolymers,⁸ was obviously caused by the hydrophilic POEGMA block.^{49,50} In the spectrum measured at 45 °C (red spectrum) the characteristic signals of the POEGMA block had not changed. However, the signals attributed to the PNIPAM

block, viz., the methine signal (denoted B) at 3.86 ppm and the methyl signal (D) at 1.10 ppm, had decreased and broadened due to dehydration. Additionally, the backbone signals from 2.20 to 1.20 ppm had flattened somewhat due to the PNIPAM backbone contribution to these peaks. The decrease of the methine proton signal (B) with temperature is shown in Figure 1B. The integrals of this peak, normalized to the value at 25 °C, are plotted in Figure 2 (black curve). During heating, the integral remains unchanged until it drops suddenly at 39 °C, where the chains lose hydration and collapse. A turbidity measurement was performed on the same solution in D₂O at a heating rate of 0.1 °C/min (blue curve in Figure 2), showing a sharp decrease of transmittance reaching 50% at 38.6 °C. It should be noted that the POEGMA block prevented a final precipitation of the phase-separated PNIPAM with the transmittance decreasing to ~2.8% at 42 °C. Most importantly, the molecular event observed by NMR, i.e. dehydration, and the macroscopic event observed by UV–vis, i.e. phase separation, occur at the same temperature. This is not unexpected;⁴⁹ PNIPAM has been receiving great attention for its sharp transition for decades,^{8,35} and NMR spectroscopy has been shown to be a suitable method for monitoring such phase transitions.^{38,39}

Solution Behavior in Alcohol. After the sharp PNIPAM LCST transition of POEGMA-*b*-PNIPAM had been confirmed in water, the solution behavior of POEGMA-*b*-PNIPAM and POEGMA-*b*-PDEAM in alcohols was investigated. First, the UCST transition of POEGMA was assessed by ¹H NMR and UV–vis spectroscopy and DLS on POEGMA-*b*-PNIPAM in (deuterated) 2-propanol. Differences in phase transition

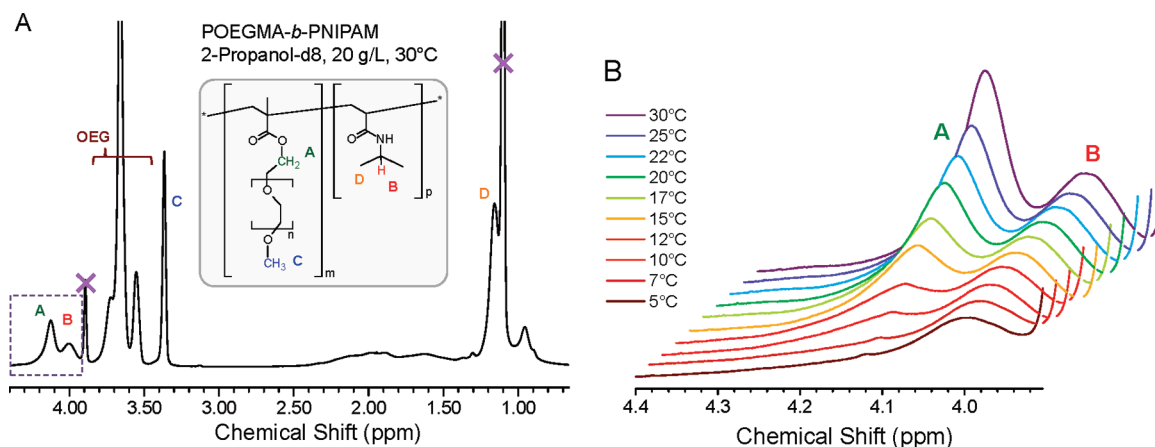


Figure 3. Variable temperature ^1H NMR measurements of POEGMA-*b*-PNIPAM in 2-propanol- d_8 . (A) Spectrum at 30 °C with assigned peaks. Residual solvent signals are crossed out. (B) Sections of spectra (dashed rectangle in part A) showing the decrease of the peak corresponding to the OEG methylene group adjacent to the ester moiety during cooling.

behavior between deuterated and nondeuterated solvents have been shown to exist for the PNIPAM- $\text{H}_2\text{O}/\text{D}_2\text{O}$ system.⁵¹ However, these differences are small, and for 2-propanol, in which the mass percentage of H/D is greatly reduced compared to $\text{H}_2\text{O}/\text{D}_2\text{O}$, the isotope effect was neglected. Figure 3 shows ^1H NMR spectra measured on a 20 g/L sample. Apart from slightly shifted resonance frequencies, the spectrum at 30 °C, shown in Figure 3A, is in good agreement with the spectra measured in D_2O at 25 °C or in CDCl_3 at 25 °C, indicating that both blocks are molecularly dissolved and fully solvated. Upon cooling the solution, a decrease of most of the signals corresponding to the POEGMA block was observed, while the PNIPAM signals did not change until cooled well below the phase separation temperature of POEGMA (vide infra). Figure 3B shows the signals of the OEG methylene group closest to the backbone, denoted A, at 4.12 ppm, and the signal of the PNIPAM methine group, denoted B, at 4.01 ppm, at variable temperatures. It can clearly be seen that the signal arising from the POEGMA block decreases with temperature, indicating the loss of solvation during the UCST-type transition. In agreement with the solubility of PNIPAM in 2-propanol even at low temperatures, signal B does not change over the monitored temperature range.

In order to gain closer insights into the transition of POEGMA in alcohols, four NMR integrals were evaluated during the cooling of POEGMA-*b*-PNIPAM. Figure 4 shows

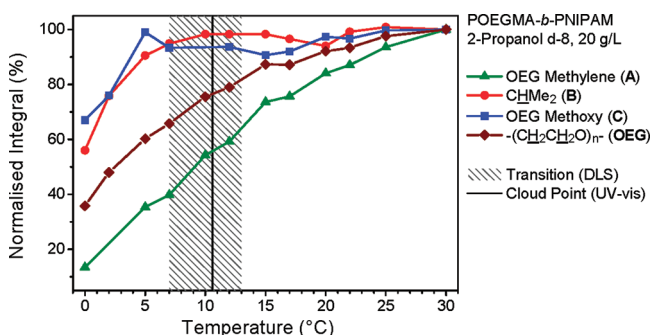


Figure 4. Normalized integrals of four NMR signals as assigned in Figure 3A in dependence of temperature; value of cloud point, and temperature regime in which a steep increase of average size was found by DLS.

the integrals, normalized to their values at 30 °C, of the signals A and B (mentioned above, green and red plot, respectively) and of the methoxy group located at the far end of the OEG side chains (denoted C, 3.36 ppm, blue plot) and of the multiplet in the range of 3.86–3.50 ppm, which corresponds to the OEG chain excluding groups A and C (denoted OEG, brown plot). Also shown in Figure 4 is the cloud point measured by UV-vis (10.6 °C, black vertical line). The turbidity measurement of the sample (shown in Figure S3 of the Supporting Information) showed a decrease of transmittance between 13 and 8 °C, indicating macroscopic phase separation and formation of aggregates. In agreement with this, DLS showed a (number-average) size increase from ~6 nm at 14 °C (unimers) to ~50 nm at 4 °C (micellar aggregates); this temperature region is shaded in Figure 4. In contrast to the PNIPAM signals in D_2O as described above, there is no sudden decrease of POEGMA integrals. From 30 °C downward, the integral of methylene group A decreases in an almost linear fashion (green curve), reaching 13% of its original value at 0 °C. Similarly, but less pronounced, the OEG integral (brown curve) also decreases gradually with decreasing temperatures with a slightly steeper slope at lower temperatures, dropping to 36% of its original value when the temperature is decreased to 0 °C. The results show the broad temperature range (spanning at least 30 °C) in which the solubility change of POEGMA takes place. This range is similar to the one observed for PMMA in ethanol/water.⁴ Surprisingly, the OEG methoxy group (C, blue curve) does not undergo desolvation when the temperature is decreased, with its integral remaining above 92% over the entire temperature region from 30 to 5 °C. As mentioned above, the PNIPAM block remains soluble in cold alcohol, and its integral (B, red curve) does not decrease from its value at 30 °C until ~5 °C. Below 5 °C, the phase-separated POEGMA cores can be expected to collapse further, thus restricting the movements and increasing the relaxation times of the PNIPAM chains causing all integrals to drop. The striking feature is that there is no obvious connection between the phase transition observed by UV-vis and DLS and the molecular events observed by ^1H NMR spectroscopy. Phase separation occurred when the integral value of group A had reached ~54% of its original value. Apart from a decrease of all integrals well below the phase separation temperature, ^1H NMR spectroscopy gives no

evidence that phase separation of the POEGMA blocks had occurred.

Similar results were obtained for the diblock copolymer POEGMA-*b*-PDEAM at a concentration of 20 g/L in (deuterated) 2-propanol (Figure 5). For this material, the

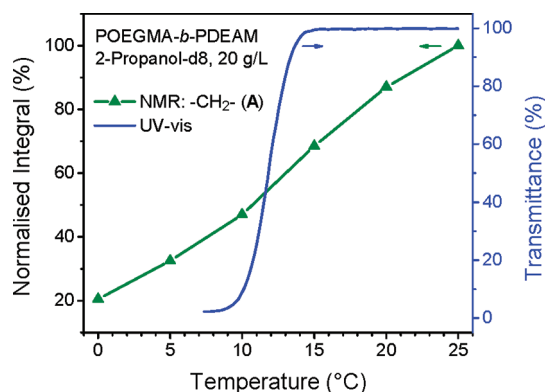


Figure 5. Cooling of POEGMA-*b*-PDEAM in 2-propanol: integral of NMR signal A (methylene group adjacent to ester linkage, green curve, left axis) and turbidity measurement (blue curve, right axis).

integral of group A also gradually decreased with decreasing temperature, unperturbed by the phase transition that was observed by turbidity at 11.8 °C. At this temperature, the integral of signal A had decreased to 55% of its value at 25 °C, showing that changing the second block did not have an impact on the solution behavior of POEGMA.

At high temperatures, where 2-propanol is a thermodynamically good solvent for POEGMA, this block can be expected to be in an expanded coil conformation with the OEG side chains extending like spokes from the backbone. The development of the integrals A, C, and OEG with decreasing temperature shows the gradual collapse of the OEG side chains onto the backbone, beginning at the ester linkage. This causes a solvation gradient along the OEG side chains which steepens with decreasing temperature as indicated by the steeper decrease of signal A compared to the OEG signal. A loss of solvent molecules in the immediate periphery of the backbone can also be expected to influence the conformation of the POEGMA chains. The theory of coil-to-globule collapse, followed by intrachain aggregation, of macromolecules in organic solvents has been extensively studied.^{52–55} The process is generally considered to follow four stages: (1) intrachain crumpling, (2) knotting of individual chains, (3) intermolecular aggregation, and (4) interchain entanglement.⁵³ During the first two stages, the overall chain dimensions decrease only slightly.⁵⁵ The experimental observation of these events is challenging. Light scattering experiments on extremely dilute samples of high molecular weight (>1000 kg/mol) have been used to confirm a crumpled globular and a compact spherical globular state of single polymer chains in a polystyrene/cyclohexane system.^{56–59} Assuming that POEGMA in 2-propanol undergoes a coil-to-globule collapse conforming with the general theory, the gradual desolvation starting ~20 °C above the phase transition can be expected to reflect the crumpling stage of the POEGMA collapse. The knotting process (stage 2) is only observed for long polymers with a high degree of polymerization above a critical value and cannot be expected to occur for the present POEGMA block.^{52,53,59} With the OEG side chains acting as a “sensor” for solvent being driven out of the

surroundings of the backbone, qualitative information on the chain conformation and the early stage chain collapse can be obtained by NMR on a polymer several orders of magnitude too small, with respect to its molecular weight, for light scattering studies. A collapse starting at the ester linkage is in contrast to previous observations on PNIPAM, suggesting that chain collapse is initiated at the mobile chain ends.⁶⁰ For POEGMA in alcohol, the enthalpic interactions between solvent and OEG chains are obviously more unfavorable in closer proximity to the ester linkage. In this context it is noteworthy that a recent study by our group⁶¹ has shown that the ester moiety in POEGMA also plays an important role in the dependence of the UCST on the value of *n* in the alcohol solvent $C_nH_{2n+1}OH$. While POEGMA displays UCST values that increase strongly with *n*, a formal replacement of the ester moieties with amide groups removes this dependence on *n*.

As mentioned in the Introduction, polymer concentration can have an enormous impact on the phase transition temperature. In Figure 6, the UCST-type cloud points of a

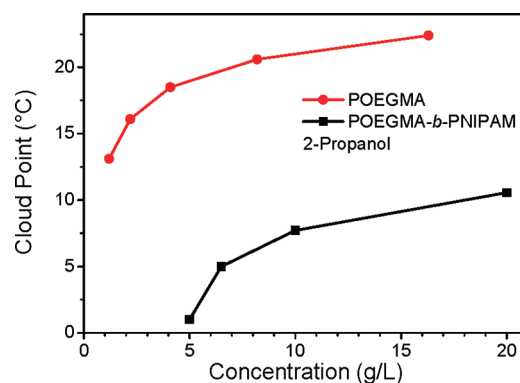


Figure 6. Concentration dependence of the phase separation of POEGMA and POEGMA-*b*-PNIPAM.

POEGMA sample, 8.7 kg/mol, taken from previous work²³ are plotted (red curve). As the concentration drops from 16.3 to 1.2 g/L, the cloud point decreases with an increasing slope, dropping by 9.3 °C from 22.4 to 13.1 °C. Also shown in Figure 6 are the cloud points measured for POEGMA-*b*-PNIPAM (black curve). The value for the 20 g/L sample, 10.6 °C, is indicated as a vertical line in Figure 4. The corresponding turbidity curves are shown in Figure S3 of the Supporting Information. It should be noted that the presence of the PNIPAM block prevented a precipitation and that the transmittance did not decrease to 0% due to the formation of large stabilized micellar aggregates. Same as homo POEGMA, POEGMA-*b*-PNIPAM displays a strong concentration-dependent UCST transition. However, the binodal is shifted toward higher concentrations with a large downward sloping occurring around 5 g/L. The presence of the PNIPAM block, enhancing the solubility and effectively diluting the POEGMA component in the solution is responsible for this difference.

The strong concentration dependence was also confirmed by DLS measurements. Figure 7 shows number-average size distributions of POEGMA-*b*-PNIPAM in 2-propanol at variable temperatures at 20 g/L (upper plot) and 5 g/L (lower plot). As mentioned above, the 20 g/L sample aggregates into micellar structures of ~50 nm diameter in the temperature range of 13–7 °C, as is indicated by the shaded area in Figure 4. The DLS curves shown in Figure 7A show this size increase. As to be

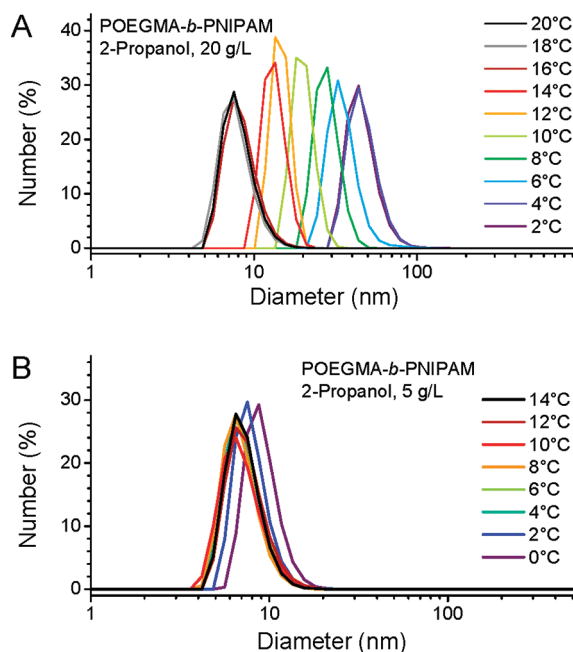


Figure 7. Number-average size distributions by DLS of POEGMA-*b*-PNIPAM in 2-propanol showing (A) a size increase due to phase separation and aggregation for a concentration of 20 g/L and (B) no formation of micellar aggregates above 0 °C for a concentration of 5 g/L.

expected for the 5 g/L sample with a much lower phase transition temperature, no such size increase was observed above 0 °C (the instrumental minimum temperature), with the size distribution indicating the presence of unimers of ~ 7 nm diameter from 14 to 4 °C. At 2 and 0 °C, the average diameter increased to 8.0 and 9.2 nm, respectively. The cloud point of this sample of ~ 1 °C is in reasonable agreement with the DLS data; differences in cooling rates or a certain temperature inaccuracy at the instrumental limit can be considered to cause the slight discrepancy.

Commonly, (co)polymers with a negligible concentration dependence on their stimulus responsive behavior are preferred—this being an important aspect in the success of PNIPAM and POEGMA in aqueous solution.¹³ With ^1H NMR spectroscopy as a qualitative tool for monitoring the early stages of chain collapse of POEGMA in 2-propanol in hand, we next investigated the UCST transition of POEGMA-*b*-PNIPAM at 5 g/L. Recall that at 20 g/L the cloud point (i.e., the phase separation) occurred at 10.6 °C when integral A had decreased to 54% of its value at 30 °C. At a concentration of 5 g/L, the cloud point was 9.6 °C lower, at ~ 1 °C. It might be expected that desolvation and the onset of the chain collapse would similarly be shifted to lower temperatures, causing interchain aggregation to occur at a similar percentage of remaining solvation than for the 20 g/L sample. Figure 8 compares the development of integrals A (green curves) and B (red curves) at a concentration of 20 g/L (light curves, open symbols) and 5 g/L (dark curves, solid symbols). All integrals were normalized to the values at 30 °C, at which temperature (apart from stronger residual solvent signals) the 5 g/L spectrum was virtually identical to the one measured at 20 g/L. Also indicated are the cloud points at 20 g/L (vertical gray line) and at 5 g/L (vertical black line). It can be seen that the concentration (within the observed range) does not impact the

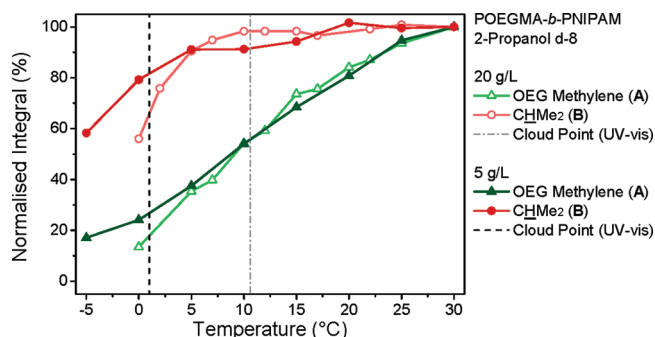


Figure 8. ^1H NMR Integrals of POEGMA methylene group (A) and PNIPAM methine group (B) in dependence of temperature at two concentrations.

gradual desolvation of the POEGMA blocks. The course of the integrals of group A is essentially identical for the two samples. At a concentration of 5 g/L, the macroscopic phase separation occurs when the ^1H NMR integral of the methylene groups adjacent to the ester linkages has decreased to $\sim 27\%$ of its value at 30 °C. The collapse of the POEGMA blocks is thus further advanced than for the 20 g/L sample before intermolecular aggregation begins. Only at temperatures below the respective phase transitions was there a difference between the spectra at 20 and 5 g/L. As mentioned above, the interchain entanglement (stage 4 of the theory mentioned above) and globule compaction reduce the mobility of the entire diblock copolymer and thus also cause the ^1H NMR signals of the soluble PNIPAM block to decrease. It can be seen in Figure 8 that for the lower concentration sample this decrease occurs at lower temperatures than for the higher concentrated sample (red curves). Below 5 °C there is also a minimal difference between the two curves of signals A which can be attributed to the fact that at this temperature the 20 g/L sample had already undergone phase separation, causing a higher degree of overlapping of broadened NMR peaks.

These results suggest that desolvation (and implied chain collapse) is a material property and, as such, independent of concentration. The macroscopic phase separation, on the other hand, involving an interchain aggregation is strongly dependent on concentration and relies on the translational diffusion, collision of (partially collapsed) chains, and subsequent segmental diffusion.^{53,62} For LCST-type transitions, complete chain collapse and phase transitions usually occur together within a narrow temperature range. Flowerlike micelles formed from telechelic hydrophobically modified PNIPAM have been shown to exhibit concentration independent dehydration temperatures above the strongly concentration-dependent cloud point temperatures.⁶³ Only on extremely dilute solutions have single chain collapses (without phase transitions) been observed.^{35,51,64–66} With the smart materials arena being dominated by LCST-type systems such as PNIPAM or POEGMA in water, the elementary differences of UCST-type transitions in polar solvents should be noted. Although the cloud points of POEGMA in alcohol show a strong concentration dependence (and even more so in the diblock copolymer), a concentration-independent chain collapse is of importance for potential applications that do not rely on a macroscopic phase separation, but rather on the overall end-to-end distance of polymer chains. Examples include an end-to-end energy transfer^{67,68} and the swelling of grafts on planar or spherical⁶⁹ surfaces or cross-linked networks.

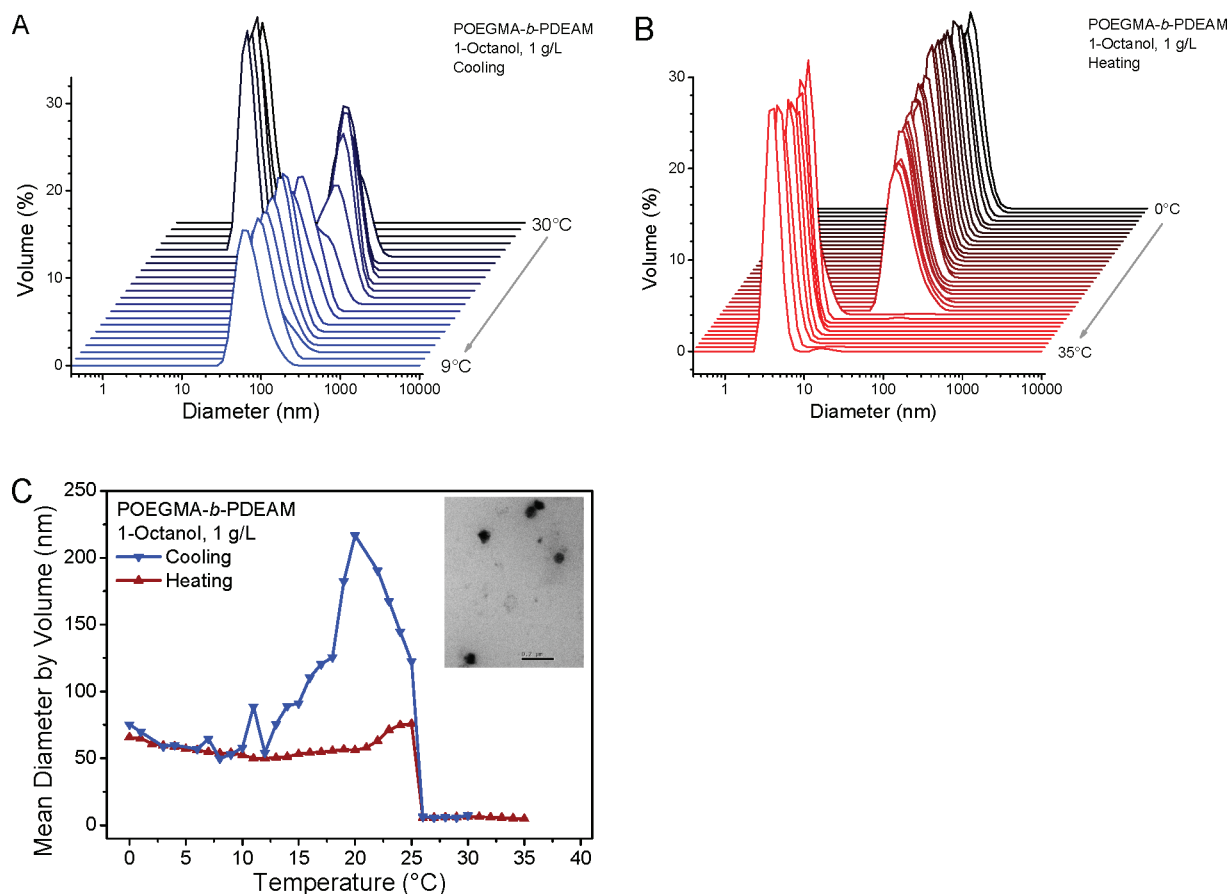


Figure 9. Self-assembly of POEGMA-*b*-PDEAM in 1-octanol monitored by DLS. Size distributions by volume during cooling (A), heating (B), and average diameters during cooling and heating in dependence of temperature (C) with a TEM image of a sample prepared at 0 °C (inset, scale bar 200 nm).

Self-Assembly. It is interesting to note that although ^1H NMR spectroscopy indicated that the gradual desolvation event for POEGMA occurs over a range of more than 30 °C, both DLS and UV-vis revealed a significantly narrow phase separation regime. This is a promising characteristic for potential self-assembly driven by a UCST phase separation. Commonly, concentrations lower than 20 g/L are used for the formation of well-defined micelles from AB diblock copolymers. For this reason, 1-octanol was used as solvent in which POEGMA has an increased UCST compared to 2-propanol. Therefore, at a lower concentration of 1 g/L, cloud points around RT could be exploited. The solubility of PNIPAM and PDEAM in 1-octanol at variable temperatures was confirmed by UV-vis and DLS (Figures S4 and S5 of the Supporting Information). Figure 9 shows the size evolution of POEGMA-*b*-PDEAM in 1-octanol during cooling (9A) and heating (9B). At 30 °C, the diblock copolymer is molecularly dissolved, and DLS shows unimers with a size of ~6.0 nm (9A). At 25 °C, the diameter abruptly jumps to a value of more than 100 nm. There was no evidence of two populations at this phase transition temperature, suggesting that the majority of chains had aggregated. With further cooling, the (volume average) diameter further increased to a maximum of over 200 nm at 20 °C (Figure 9C). We attribute this to the formation of loosely aggregated clusters due to the fact that the POEGMA component is still solvated to a certain degree at this stage. In agreement with ^1H NMR measurements in 2-propanol- d_8 which suggested a further compaction of aggregates below

the cloud point, DLS showed a diameter decrease upon further cooling to ~12 °C, below which a diameter of ~60 nm was observed (9A and 9C). This was attributed to the formation of micelles retaining a certain amount of solvent in their cores. Polydispersity indices (averaged from three DLS measurements at each temperature) ranged from 0.039 to 0.102 in the region of 0–10 °C, indicating micelles with a well-defined size distribution. TEM recorded of a sample dried at 0 °C (inset in Figure 9C) confirmed the presence of spherical aggregates of a similar diameter.

Upon heating, a different pathway was observed (9B). The diameter of the formed micelles stayed essentially constant, with a slight increase just before the dissolution into unimers at 25 °C. This suggests that a hysteresis similar to that found for LCST polymers^{51,64} exists for POEGMA in alcohols. The POEGMA cores of the micelles stay intact and swell only slightly upon heating. Surprisingly, the disappearance and reformation of unimers occurred at 25 °C upon cooling and heating, respectively, showing no hysteresis of phase transition temperature. At 26 and 27 °C, a small population of micelles (less than 0.5 vol %) remained with the rest of the material being molecularly dissolved. These results show that defined micellar structures can indeed be obtained by exploiting the UCST transition of POEGMA in alcohols. However, due to the gradual transition from soluble to insoluble, cooling to a temperature ~15 °C below the phase separation temperature was required to produce compact particles. These particles are

then stable during heating, redissolving at a predetermined temperature.

CONCLUSION

The UCST transition of POEGMA in alcohols was investigated in detail by comparison of the solution behavior of the double thermoresponsive diblock copolymers POEGMA-*b*-PNIPAM and POEGMA-*b*-PDEAM in water and alcohols. In water, chain collapse and macroscopic phase separation of PNIPAM occurred together. In alcohol, the transition from soluble to insoluble for POEGMA during cooling occurred very gradually, with solvent being driven out of the periphery of the backbone over a range of ~ 30 °C, indicating early stages of chain crumpling. The transition from soluble to insoluble was independent of concentration within a concentration range that strongly influences the macroscopic phase separation (cloud point). Below the phase separation, the ongoing desolvation caused a further compaction of aggregates, thus reducing overall polymer mobility and effecting aggregate diameters to decrease. During the heating of aggregates only a slight swelling was observed. The results suggest that for POEGMA in alcohol macroscopic phase separation and microscopic chain solvation and conformation should be treated separately. The narrow phase separation temperature and complete redissolution of aggregates are promising for the self-assembly of diblock copolymers leading to inverted structures with hydrophilic POEGMA cores.

ASSOCIATED CONTENT

Supporting Information

SEC traces of all polymers, ^{19}F NMR measurements, cloud point curves of POEGMA-*b*-PNIPAM in 2-propanol at varying concentration, DLS, and UV-vis measurements of PNIPAM and PDEAM in 1-octanol. This material is available free of charge via the Internet at <http://pubs.acs.org>.

AUTHOR INFORMATION

Corresponding Author

*E-mail: a.lowe@unsw.edu.au (A.B.L.); t.davis@unsw.edu.au (T.P.D.).

Notes

The authors declare no competing financial interest.

ACKNOWLEDGMENTS

P.J.R. kindly acknowledges Dr. Douglas Lawes of the Nuclear Magnetic Resonance Facility for help with variable temperature NMR measurements.

REFERENCES

- (1) Gil, E. S.; Hudson, S. M. *Prog. Polym. Sci.* **2004**, *29*, 1173.
- (2) Wei, H.; Cheng, S.-X.; Zhang, X.-Z.; Zhuo, R.-X. *Prog. Polym. Sci.* **2009**, *34*, 893.
- (3) Uchiyama, S.; Kawai, N.; de Silva, A. P.; Iwai, K. *J. Am. Chem. Soc.* **2004**, *126*, 3032.
- (4) Pietsch, C.; Hoogenboom, R.; Schubert, U. S. *Polym. Chem.* **2010**, *1*, 1005.
- (5) Pietsch, C.; Hoogenboom, R.; Schubert, U. S. *Angew. Chem., Int. Ed.* **2009**, *48*, 5653.
- (6) Li, C.; Gunari, N.; Fischer, K.; Janshoff, A.; Schmidt, M. *Angew. Chem., Int. Ed.* **2004**, *43*, 1101.
- (7) Mori, T.; Umeno, D.; Maeda, M. *Biotechnol. Bioeng.* **2001**, *72*, 261.
- (8) Schild, H. G. *Prog. Polym. Sci.* **1992**, *17*, 163.
- (9) Idziak, I.; Avoce, D.; Lessard, D.; Gravel, D.; Zhu, X. X. *Macromolecules* **1999**, *32*, 1260.
- (10) Hu, Z.; Cai, T.; Chi, C. *Soft Matter* **2010**, *6*, 2115.
- (11) Lutz, J.-F. *Adv. Mater.* **2011**, *23*, 2237.
- (12) Lutz, J.-F. *J. Polym. Sci., Part A: Polym. Chem.* **2008**, *46*, 3459.
- (13) Lutz, J.-F.; Akdemir, Ö.; Hoth, A. J. *Am. Chem. Soc.* **2006**, *128*, 13046.
- (14) Kudaibergenov, S.; Jaeger, W.; Laschewsky, A. In *Supramolecular Polymers Polymeric Betains Oligomers*; Springer: Berlin, 2006; Vol. 201, p 157.
- (15) Monroy Soto, V. M.; Galin, J. C. *Polymer* **1984**, *25*, 254.
- (16) Nagaoka, H.; Ohnishi, N.; Eguchi, M. US Patent 7847047 B2, Chisso Corporation, Osaka, Japan, 2010.
- (17) Ohnishi, N.; Furukawa, H.; Kataoka, K.; Katsuhiko, U. US Patent 7195925 B2, National Institute of Advanced Industrial Science and Technology, Chisso Corporation, 2007.
- (18) Glatzel, S.; Laschewsky, A.; Lutz, J.-F. *Macromolecules* **2011**, *44*, 413.
- (19) Seuring, J.; Bayer, F. M.; Huber, K.; Agarwal, S. *Macromolecules* **2011**, *45*, 374.
- (20) Hoogenboom, R.; Rogers, S.; Can, A.; Becer, C. R.; Guerrero-Sanchez, C.; Wouters, D.; Hoepfener, S.; Schubert, U. S. *Chem. Commun.* **2009**, 5582.
- (21) Hoogenboom, R.; Lambermont-Thijs, H. M. L.; Jochems, M. J. H. C.; Hoepfener, S.; Guerlain, C.; Fustin, C.-A.; Gohy, J.-F.; Schubert, U. S. *Soft Matter* **2009**, *5*, 3590.
- (22) Hoogenboom, R.; Thijs, H. M. L.; Wouters, D.; Hoepfener, S.; Schubert, U. S. *Soft Matter* **2008**, *4*, 103.
- (23) Roth, P. J.; Jochum, F. D.; Theato, P. *Soft Matter* **2011**, *7*, 2484.
- (24) Weaver, J. V. M.; Armes, S. P.; Büttin, V. *Chem. Commun.* **2002**, 2122.
- (25) Büttin, V.; Liu, S.; Weaver, J. V. M.; Bories-Azeau, X.; Cai, Y.; Armes, S. P. *React. Funct. Polym.* **2006**, *66*, 157.
- (26) Arotcarena, M.; Heise, B.; Ishaya, S.; Laschewsky, A. *J. Am. Chem. Soc.* **2002**, *124*, 3787.
- (27) Virtanen, J.; Arotcarena, M.; Heise, B.; Ishaya, S.; Laschewsky, A.; Tenhu, H. *Langmuir* **2002**, *18*, 5360.
- (28) Maeda, Y.; Mochiduki, H.; Ikeda, I. *Macromol. Rapid Commun.* **2004**, *25*, 1330.
- (29) Dimitrov, I.; Trzebicka, B.; Müller, A. H. E.; Dworak, A.; Tsvetanov, C. B. *Prog. Polym. Sci.* **2007**, *32*, 1275.
- (30) Chang, Y.; Chen, W.-Y.; Yandi, W.; Shih, Y.-J.; Chu, W.-L.; Liu, Y.-L.; Chu, C.-W.; Ruaan, R.-C.; Higuchi, A. *Biomacromolecules* **2009**, *10*, 2092.
- (31) Bai, Z.; He, Y.; Young, N. P.; Lodge, T. P. *Macromolecules* **2008**, *41*, 6615.
- (32) Lee, H.-N.; Bai, Z.; Newell, N.; Lodge, T. P. *Macromolecules* **2010**, *43*, 9522.
- (33) Boyer, C.; Stenzel, M. H.; Davis, T. P. *J. Polym. Sci., Part A: Polym. Chem.* **2011**, *49*, 551.
- (34) Rubinstein, M.; Colby, R. E. *Polymer Physics*; Oxford University Press: New York, 2003; Chapter 4.
- (35) Ding, Y.; Ye, X.; Zhang, G. *J. Phys. Chem. B* **2008**, *112*, 8496.
- (36) Neugebauer, D. *Polym. Int.* **2007**, *56*, 1469.
- (37) Starovoytova, L.; Spěváček, J.; Hanyková, L.; Ilavský, M. *Polymer* **2004**, *45*, 5905.
- (38) Zeng, F.; Tong, Z.; Feng, H. *Polymer* **1997**, *38*, 5539.
- (39) Deshmukh, M. V.; Vaidya, A. A.; Kulkarni, M. G.; Rajamohanam, P. R.; Ganapathy, S. *Polymer* **2000**, *41*, 7951.
- (40) Vamvakaki, M.; Palioura, D.; Spyros, A.; Armes, S. P.; Anastasiadis, S. H. *Macromolecules* **2006**, *39*, 5106.
- (41) Yaws, C. L. *Chemical Properties Handbook*; McGraw-Hill: New York, 1999; Chapter 22.
- (42) Matsuo, S.; Makita, T. *Int. J. Thermophys.* **1989**, *10*, 833.
- (43) Mitsukami, Y.; Donovan, M. S.; Lowe, A. B.; McCormick, C. L. *Macromolecules* **2001**, *34*, 2248.
- (44) Eberhardt, M.; Mruk, R.; Zentel, R.; Théato, P. *Eur. Polym. J.* **2005**, *41*, 1569.

- (45) Jochum, F. D.; Roth, P. J.; Kessler, D.; Theato, P. *Biomacromolecules* **2010**, *11*, 2432.
- (46) Boyer, C.; Granville, A.; Davis, T. P.; Bulmus, V. J. *Polym. Sci., Part A: Polym. Chem.* **2009**, *47*, 3773.
- (47) Hoyle, C. E.; Lowe, A. B.; Bowman, C. N. *Chem. Soc. Rev.* **2010**, *39*, 1355.
- (48) Lowe, A. B. *Polym. Chem.* **2010**, *1*, 17.
- (49) Zhang, W.; Shi, L.; Wu, K.; An, Y. *Macromolecules* **2005**, *38*, 5743.
- (50) Roth, P. J.; Jochum, F. D.; Forst, F. R.; Zentel, R.; Theato, P. *Macromolecules* **2010**, *43*, 4638.
- (51) Wang, X.; Wu, C. *Macromolecules* **1999**, *32*, 4299.
- (52) Grosberg, A. Y.; Nechaev, S. K.; Shakhnovich, E. I. *J. Phys. (Paris)* **1988**, *49*, 2095.
- (53) Grosberg, A. Y.; Kuznetsov, D. V. *Macromolecules* **1993**, *26*, 4249.
- (54) Baysal, B. M.; Karasz, F. E. *Macromol. Theory Simul.* **2003**, *12*, 627.
- (55) Halperin, A.; Goldbart, P. M. *Phys. Rev. E* **2000**, *61*, 565.
- (56) Chu, B.; Yu, J.; Wang, Z.; Ewen, B.; Fischer, E.; Fytas, G., Eds.; Springer: Berlin, 1993; Vol. 91, p 142.
- (57) Chu, B.; Ying, Q.; Grosberg, A. Y. *Macromolecules* **1995**, *28*, 180.
- (58) Yu, J.; Wang, Z.; Chu, B. *Macromolecules* **1992**, *25*, 1618.
- (59) Aseyev, V.; Tenhu, H.; Winnik, F.; Temperature Dependence of the Colloidal Stability of Neutral Amphiphilic Polymers in Water. In *Conformation-Dependent Design of Sequences in Copolymers II*; Khoklov, A. R., Ed.; Springer: Berlin, 2006; Vol. 196, p 1.
- (60) Chung, J. E.; Yokoyama, M.; Aoyagi, T.; Sakurai, Y.; Okano, T. *J. Control. Release* **1998**, *53*, 119.
- (61) Chua, G. B. H.; Roth, P. J.; Duong, H. T. T.; Davis, T. P.; Lowe, A. B. *Macromolecules* **2012**, *45*, 1362.
- (62) Piçarra, S.; Gomes, P. T.; Martinho, J. M. G. *Macromolecules* **2000**, *33*, 3947.
- (63) Kujawa, P.; Segui, F.; Shaban, S.; Diab, C.; Okada, Y.; Tanaka, F.; Winnik, F. M. *Macromolecules* **2006**, *39*, 341.
- (64) Wang, X.; Qiu, X.; Wu, C. *Macromolecules* **1998**, *31*, 2972.
- (65) Wu, C.; Wang, X. *Phys. Rev. Lett.* **1998**, *80*, 4092.
- (66) Xu, J.; Zhu, Z.; Luo, S.; Wu, C.; Liu, S. *Phys. Rev. Lett.* **2006**, *96*, 027802.
- (67) Roth, P. J.; Haase, M.; Basche, T.; Theato, P.; Zentel, R. *Macromolecules* **2010**, *43*, 895.
- (68) Hong, S. W.; Kim, D. Y.; Lee, J. U.; Jo, W. H. *Macromolecules* **2009**, *42*, 2756.
- (69) Jeong, N. S.; Brebis, K.; Daniel, L. E.; O'Reilly, R. K.; Gibson, M. I. *Chem. Commun.* **2011**, *47*, 11627.